

Emulsifier-Free Emulsion Copolymerization of Styrene with Two Different Amino-Containing Cationic Monomers. I. Kinetic Studies

F. GANACHAUD, F. SAUZEDDE, A. ELAÏSSARI, C. PICHOT

Unité Mixte CNRS/bioMérieux, UMR 103, ENS-Lyon, 46 Allée d'Italie, 69364 Lyon cedex 07, France

Received 7 July 1996; accepted 25 November 1996

ABSTRACT: The kinetics of emulsifier-free emulsion copolymerization of styrene were investigated in the presence of two amino-containing monomers, aminoethyl methacrylate hydrochloride (AEMH) and vinyl benzyl amine hydrochloride (VBAH), using 2,2'-azobis(2-amidinopropane) dihydrochloride (V50) as a cationic initiator. At first the partition coefficient of AEMH and VBAH in a water-styrene mixture were measured, indicating a strong hydrophilicity for both monomers; kinetics of solution homopolymerization, as followed by $^1\text{H-NMR}$, in water provided high $k_p/k_t^{1/2}$ values at 4.0 and 1.75 ($\text{L mol}^{-1} \text{s}^{-1}$) $^{1/2}$ for AEMH and VBAH, respectively. The two monomers were found to similarly affect the kinetics of emulsion copolymerization of styrene: the overall polymerization rate and particle number increased dramatically upon increasing the functional monomer concentration; the average number of radicals per particle (\bar{n}) was dependent upon the particle size, reaching a 0.5 value for particle size below 100 nm; and the molecular weight of polymer samples decreased with the functional monomer concentration, revealing the strong activity of VBAH and AEMH in the chain transfer. The polymerization mechanism in the presence of VBAH and AEMH was discussed, referring to the coagulation nucleation mechanism to explain the formation of a large particle number. Using the method proposed by Gilbert et al., transfer rate constants were determined for each monomer (around $10 \text{ L mol}^{-1} \text{s}^{-1}$) and styrene ($4.5 \cdot 10^{-2} \text{ L mol}^{-1} \text{s}^{-1}$). © 1997 John Wiley & Sons, Inc. *J Appl Polym Sci* **65**: 2315–2330, 1997

Key words: soap-free emulsion copolymerization; styrene; amino-containing monomers; transfer rate constants; transfer mechanism

INTRODUCTION

Functional polymer latexes prepared by emulsion polymerization have received increasing attention due to their interest as model colloids for academic research investigation of various colloidal phenomena,^{1–4} for numerous industrial applications as binders (paints, adhesives, textiles, etc.) or solid phase supports in catalysis,^{5,6} and in the biomedical field (diagnostic assays,^{7,8} cell separation,⁹ drug delivery systems, etc.).

For such applications the incorporation of surface functional groups on the latex particles is of paramount importance and various strategies have been proposed for this purpose.¹⁰ The general tendency is to adequately select the nature and concentration of some ingredients involved in the polymerization recipe, for example, the initiator (which may provide functional groups upon decomposition), a given monomer or macromonomer containing a reactive group, an emulsifier (reactive surfactants were found to offer quite a versatile alternative because covalent attachment of the functionality can be imparted,¹¹ and the modification of preformed particles.^{1,6}

For many reasons, the second method was actu-

Correspondence to: Dr. C. Pichot.

ally mostly developed in emulsion polymerization, because copolymerization is always a very unique route for better control of the colloidal and molecular properties in emulsion polymers. Moreover, the availability or the design of many functional monomers allows the surface incorporation of functional groups that can be ionogenic (acidic or basic) like carboxylic^{7,14} or amino^{14,15} groups, ionic like sulfate⁴ and quaternary ammonium^{5,6} groups, or nonionic like hydroxyl or epoxy groups or a polyethylene oxide compound.¹⁶ Furthermore, due to the stability conferred by such polar or ionic groups, emulsion polymerization can be performed without the presence of an emulsifier in the final latex and generally leads to the production of monodisperse particles.

In the case of copolymerizations of a main monomer (styrene for instance) with a functional monomer, many studies were focused on the effect of the type and concentration of the functional monomers on the polymerization kinetics and mechanism^{5,17} or the colloidal and surface properties of the final particles.^{5,7,14} The chemical structure of the functional monomer plays a critical role¹⁸ in the polymerization mechanism in heterogeneous media, especially during the nucleation period (water-phase polymerization)⁵ and consequently on the final particle properties.

As part of a program to prepare well-characterized reactive particles, this article reports on the use of two different amino-containing monomers, aminoethyl methacrylate hydrochloride (AEMH) and vinyl benzyl amine hydrochloride (VBAH) in emulsifier-free copolymerization of styrene. At first, differences in partitioning and solution polymerization behavior of each functional monomer are examined. Then, a kinetic study of the soap-free emulsion copolymerization with styrene is developed with special attention on the effect of the comonomer concentration on the polymerization rate, final conversion, particle size, and the molecular weight distribution (MWD). Finally, the polymerization mechanism in the presence of such highly water-soluble comonomers is discussed.

EXPERIMENTAL

Materials and Measurements

Unless stated otherwise, reagents and solvents were used as received. Water was of milliQ grade (Millipore SA, France) and was boiled for 1 h under a nitrogen stream before used. Styrene (Jans-

sen Chemica, France) was distilled under reduced pressure; 2,2'-azobis(2-amidinopropane) dihydrochloride (V50), kindly provided by Wako Chemical GmbH (Germany), was recrystallized from a 50/50 weight water/acetone mixture. AEMH (Kodak) was used as received. VBAH was obtained by precipitating vinyl benzyl amine (synthesized according to Delair et al.¹⁵) in an HCl 1N pentane solution. The two ionic monomer formulae and their corresponding ¹H-NMR assignments are given in Figure 1.

The ¹H-NMR spectra were recorded on a Bruker AC 200 spectrometer, with deuterated trimethyl siloxane sodium propionate (Tspd₄) (from SDS) as an internal reference. Particle sizes were determined by transmission electron microscopy (TEM) with Hitachi equipment at the CMABO Université Claude Bernard, Lyon. For each latex approximately 50 particles were measured with a Hewlett-Packard 911 A Digitalyzer. Gel permeation chromatography (GPC) was carried out with a Waters device equipped with microstyrigel columns (porosity 10², 5 × 10², 10³, and 10⁴); the eluent was THF (flow rate of 1 mL min⁻¹), and detection was performed by measurement of the optical density at 253 nm (using a Waters 484 UV spectrometer detector). Number (\overline{M}_n) and weight (\overline{M}_w) average molecular weights, as well as the polydispersity index (I_p) are defined as

$$\overline{M}_n = \frac{\sum N_i M_i}{\sum N_i} = \sum n_i M_i \quad (1)$$

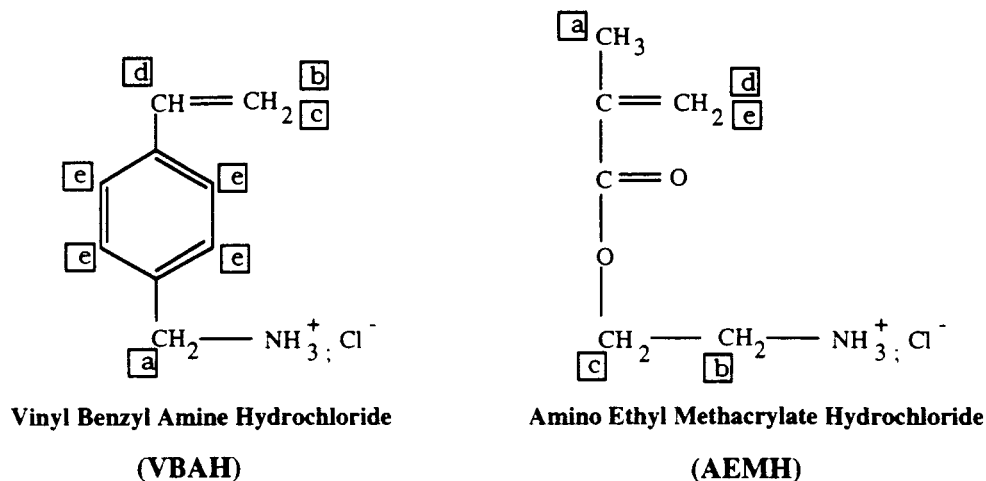
$$\overline{M}_w = \frac{\sum N_i M_i^2}{\sum N_i M_i} = \sum c_i M_i \quad (2)$$

$$I_p = \frac{\overline{M}_w}{\overline{M}_n} \quad (3)$$

where N_i is the number of species i of molecular weight M_i . These parameters were derived from a calibration using narrowly distributed polystyrene standards.

Partition Coefficients

Partition coefficients were experimentally determined with a gravimetric method. Ten milliliters of water (M_{wat}) and 1 mL of styrene (M_{St}) were accurately weighed. Various amounts of functional monomer were weighed (M_j), ranging from 0.015 to 0.6 g, and each was introduced in a water/styrene mixture (90/10 weight). After shaking



¹H-NMR (D₂O) VBAH : d = 4.05 (s; 2H; a), 5.25 (d; 1H; b), 5.77 (d; 1H; c), 6.70 (dd; 1H; d), 7.33 (m; 4H; e).

¹H-NMR (D₂O) AEMH : d = 1.95 (s; 3H; a), 3.41 (t; 2H; b), 4.45 (t; 2H; c), 5.78 (s; 1H; d), 6.20 (s; 1H; e).

Figure 1 Monomer formulae and corresponding ¹H-NMR chemical shifts.

until the monomers were entirely solubilized, the emulsion was poured into a separating funnel. When the aqueous phase was clear, a sample from this phase was weighed and dried in a vacuum. Then the residue was weighed, corresponding to the monomer amount in the aqueous phase.

From the dried mass, the monomer fraction amount in the aqueous phase $F_{j\text{wat}}$ can be deduced from

$$F_{j\text{wat}} = \frac{M_{j\text{wat}}}{M_{\text{wat}}} \quad (4)$$

Then by difference with the initial amount M_j introduced in the system, the monomer fraction quantity ($F_{j\text{st}}$) in the styrene phase can be calculated.

$$F_{j\text{st}} = \frac{M_j - M_{j\text{wat}}}{M_{\text{st}}} \quad (5)$$

Finally, the partition coefficient K_s is defined as the saturated value of the molar coefficient calculated as

$$K_s = \lim_{M_j \rightarrow \infty} (K) \quad \text{with} \quad K = \frac{F_{j\text{wat}}/MM_{\text{wat}}}{F_{j\text{st}}/MM_{\text{st}}} \quad (6)$$

with MM_{wat} and MM_{st} being the water and styrene molecular weights (18 and 104 g mol⁻¹ respectively).

Solution Polymerization

Radical homopolymerization of each monomer was carried out in water solution at 60°C under the same experimental conditions. The recipe used for each monomer is given in Table I. Kinetics were directly monitored in the tube by ¹H-NMR spectrometry.¹⁹

Kinetics of AEMH polymerization was achieved by following the variation with time of the ratio of the vinyl proton peak areas at 5.78 and 6.20

Table I Recipes of VBAH and AEMH Solution Polymerizations with V50 as Initiator

Reagents	Concn (mol L ⁻¹)
AEMH/VBAH	0.1
V50 ^a	5 × 10 ⁻³
Tspd ₄ ^b	10 ⁻²

^a Initiator.

^b Only for VBAH recipe.

ppm versus the methylene proton peak area at 3.41 ppm (Fig. 1). The latter peak area remained constant throughout the polymerization reaction; therefore, it could be used as an internal standard to assess the consumption of the vinyl protons during the polymerization process.

In the case of VBAH, the only methylene peak located at 4.05 ppm was masked by the water peak, strongly shifted at 60°C; kinetic measurements were then performed by integrating the vinyl proton peak areas at 5.25 and 5.77 ppm versus the peak area of Tspd₄ that was used as an internal standard (peak located at 0 ppm).

In each case, average conversion values and experimental errors were calculated from the two integrated peak areas.

Preparation of Cationic Polystyrene Latexes

The polymerizations were performed batchwise in a thermostated reactor under a nitrogen atmosphere. The required amount of water and styrene were brought to 70°C and left for 30 min, stirring at 300 rpm, while purging with nitrogen to remove the oxygen; the theoretical solid content was around 10%. Then the comonomer (AEMH or VBAH) was dissolved in about 2 mL of water and it was added into the reaction mixture. The polymerization reaction started with the introduction of a solution of 0.32 g of the initiator (V50) in 2 mL of water. Reactions were run for 20 h at 70°C and the overall conversion, referring to the styrene, was determined by thermogravimetry.

Polymerization Kinetics

The polymerization rates (R_p in mol L⁻¹ s⁻¹) were deduced from the conversion and time curves obtained during the particle growth. Then R_p was related to the particle number by eq. (7), according to the Smith–Ewart theory²⁰:

$$R_p = k_p \times [M] \times \frac{N_p}{N_A} \times \bar{n} \quad (7)$$

where k_p is the propagation rate constant (L mol⁻¹ s⁻¹), $[M]$ is the monomer concentration in the particles (mol L⁻¹), N_A is the Avogadro number, \bar{n} is the average radical number in the particles (stated to be 0.5 if zero-one conditions are postulated), and N_p is the particle number per volume unit of latex (L⁻¹) defined by the following relation:

$$N_p = \frac{6 \cdot \text{SC}}{\rho \cdot \pi \cdot \bar{D}_n^3} \quad (8)$$

here SC is the solid content (g L⁻¹), ρ is the polystyrene density (1.045 g cm⁻³), and \bar{D}_n is the number average particle diameter (cm) as measured by TEM. R_p and N_p were experimentally obtained. Taking $k_p = 4.8 \cdot 10^2$ L mol⁻¹ s⁻¹ and $[M] = 5.8$ mol L⁻¹,^{21,22} the average radical numbers per particle, \bar{n} , can be calculated for the different systems and compared to a value postulated in the zero-one conditions (0.5).

Particle Size and Size Distribution

Particle sizes and distribution were determined by TEM. A computer program analyzed the data to calculate the number (\bar{D}_n) and weight (\bar{D}_w) average diameters of the latex particles as defined by

$$\bar{D}_n = \frac{\sum N_i D_i}{\sum N_i} \quad (9)$$

$$\bar{D}_w = \left(\frac{\sum N_i D_i^6}{\sum N_i D_i^3} \right)^{1/3} \quad (10)$$

where N_i is the number of species i of diameter D_i . The polydispersity (\bar{U}) was defined by

$$\bar{U} = \frac{\bar{D}_w}{\bar{D}_n} \quad (11)$$

RESULTS

Physicochemical Properties of Ionic Monomers

Two main pertinent parameters were considered to explain the emulsifier-free emulsion polymerization of styrene kinetics in the presence of AEMH or VBAH: the monomer partition coefficients between water and styrene and its variation as polymerization proceeds and the polymerizability of the monomer in solution polymerization in water.

Partitioning in Organic/Water Diphasic Medium

Both monomer partition coefficients²³ between water and St media were calculated at 25°C as described in the Experimental section. The molar partition coefficient versus the monomer amount

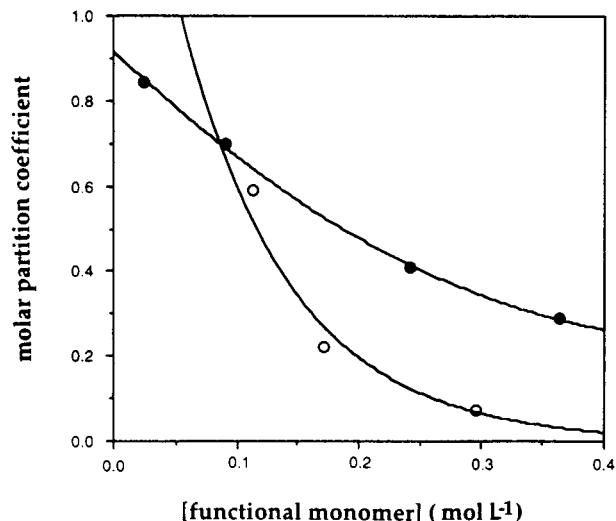


Figure 2 Partition coefficient of (○) VBAH and (●) AEMH according to eq. (1).

curve is given in Figure 2. From these results, two main remarks may be emphasized.

1. Molar partition coefficients are relatively high, which indicates that each monomer is rather more soluble in water than in St, as expected. Furthermore, the K_s value depends on the monomer amount introduced in solution, until the two phases are in equilibrium; the plateau values are then $K_s = 0.07$ and 0.28 for VBAH and AEMH, respectively.
2. The curve slope decreases more rapidly for VBAH than for AEMH, which means that the monomer partition value $K_{s(\text{VBAH})}$ is reached for smaller monomer amounts. Then, although VBAH is strongly water soluble, it exhibits a higher affinity for the organic phase than AEMH.

Solution Polymerization

Kinetics of solution polymerization were examined to estimate the polymerizability of both ionic monomers in water. VBAH and AEMH homopolymerizations were carried out at 60°C in deuterium oxide (D₂O), using V50 as the initiator. The recipe is given in Table I. As previously mentioned in the experimental part, kinetics were followed directly by ¹H-NMR, which provided a quantitative assessment of the residual monomer amount.

Kinetic data are reported in Figure 3(a) as a conversion versus time plot. A very high polymerization rate (R_p) is clearly observed in both cases (the reactions were completed within about 30 min); R_p was significantly faster with AEMH. These data were used to determine the so-called $k_p/k_t^{1/2}$ ratio from the well-known equation,

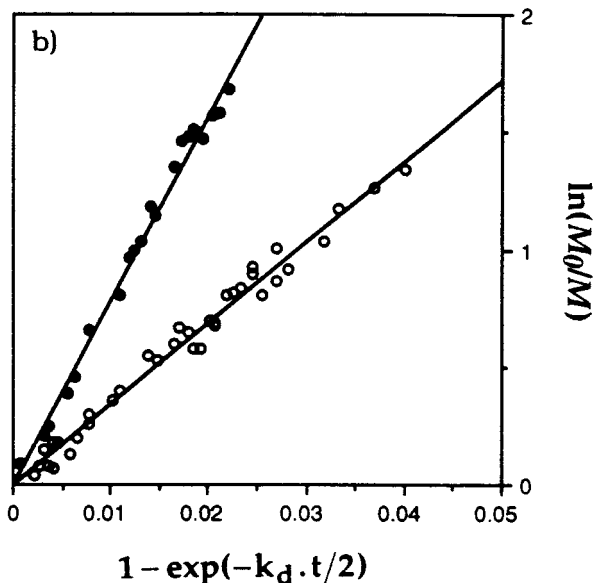
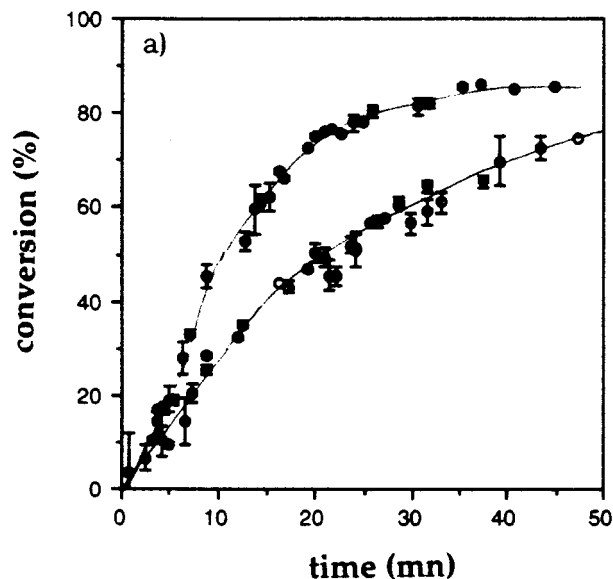


Figure 3 (a) Conversion versus time for solution polymerizations of (○) VBAH and (●) AEMH in water, with V50 as the initiator. Polymerization temperature: 60°C. (b) $\ln([M_0]/[M])$ versus $(1 - e^{-k_d \cdot t/2})$ plots for (○) VBAH and (●) AEMH obtained from solution polymerization in water.

Table II $k_p/k_t^{1/2}$ Values for Two Functional Monomers and Corresponding Original Monomers

Monomer	$k_p/k_t^{1/2}$ (L mol ⁻¹ s ⁻¹) ^{1/2}	k_p L mol ⁻¹ s ⁻¹	k_t 10 ⁶ L mol ⁻¹ s ⁻¹
VBAH ^a	1.75 ± 0.05	—	—
AEMH ^a	4.0 ± 0.1	—	—
VBA ^b	0.025	—	—
Styrene ^c	0.02	176	72
MMA ^c	0.06	290	21

^a This work.^b In toluene, with AIBN as the initiator.²⁶^c Determination with pulse laser frequency.²⁵

$$\ln([M_0]/[M]) = 2(k_p/k_t^{1/2})(2f \cdot [I_0]/k_d)^{1/2}(1 - e^{-k_d \cdot t/2}) \quad (12)$$

where $[M_0]$ and $[M]$ are the monomer concentrations at times $t = 0$ and t , respectively; $[I_0]$ is the initial initiator concentration; k_p and k_t are the propagation and termination rate constants, respectively; and k_d and f are the decomposition rate and initiator efficiency, respectively. A plot of $\ln([M_0]/[M])$ versus $(1 - e^{-k_d \cdot t/2})$ is illustrated in Figure 3(b), considering $k_d = 3.32 \times 10^{-5} \text{ s}^{-1}$ for V50 at 60°C in water²⁴ and the $f = 0.5$.

The $k_p/k_t^{1/2}$ values, deduced from the slope of the obtained curves, are reported in Table II.²⁵ Under ionic form, these monomers exhibit higher polymerizability than the nonionic corresponding ones, which can be explained by inductive or mesomeric effects on the double-bond reactivity. Furthermore, $k_p/k_t^{1/2}$ for AEMH is twice that of VBAH²⁶; this could be due to the higher reactivity of methyl methacrylate (MMA) compared to St together with a lower termination constant (see k_p and k_t values for styrene and MMA in Table II). Such a difference in the ratio may also be expected in the case of ionic monomers.

Emulsifier-Free Emulsion Polymerizations

As summarized in Table III, similar recipes were used to perform soap-free emulsion polymerization of styrene with VBAH or AEMH as comonomer. The amount of ionic initiator, V50, was chosen to ensure electrostatic stabilization of the final latexes, especially for the experiment carried out in the absence of functional monomer,² as well as to keep the ionic strength almost constant. Special attention was paid to the influence of the functional monomer amount on the polymerization

rate, the particle number created at the very beginning of the polymerization, the final particle sizes, and the overall conversion. Furthermore, average molecular weights with conversion were measured.

Influence of Ionic Comonomers on Polymerization Rate

Conversion versus time curves for emulsion polymerization of styrene, using four different concentrations of VBAH, are reported in Figure 4, showing a dramatic effect of the ionic monomer on the kinetics and final conversion. A plot of the initial rate of polymerization versus the ionic comonomer concentration exhibits a linear relationship as illustrated in Figure 5. Contrary to what was previously observed in solution, it was not possible to evidence any difference between AEMH and VBAH on the overall polymerization rate. Indeed, these curves were determined gravimetrically with some uncertainty due to the fast polymerization process. Such an increase in the polymerization rate resulting from the introduction of small amounts of ionic monomer might

Table III Recipes Used in Soap-Free Batch Polymerization of AEMH and VBAH

Reagents	Quantities (g)
Water	200
Styrene	20
AEMH/VBAH ^a	Variable (between 0 and 0.32)
V50 ^b	0.32

2,2'-Azobis(2-amidino propane) hydrochloride (V50) as initiator; reaction temperature 70°C; stirring rate 300 rpm.

^a Molar ratio.^b Initiator.

emphasize the higher ability of such monomer to increase the final particle numbers than when only styrene is polymerized [eq. (7)]. This is a general trend widely reported in the case of many other ionic monomers.^{27,28}

Influence of Ionic Comonomers on Particle Number

The particle size data and polydispersity index deduced from TEM measurements are given in Table IV. It is clear that the particle size decreased upon increasing the ionic monomer concentration. Moreover, the latexes were rather monodisperse, except when the initial monomer concentration was set too high. (In that case large amounts of polyelectrolytes were produced, which favors secondary nucleation, as already suggested in the literature.⁵) Particle numbers were estimated according to eq. (8).

Figure 6, plotted in a log scale, shows the influence of the cationic monomer concentration on the final particle number. The above-mentioned trend was clearly confirmed and a linear relationship was obtained; however, no detectable difference was found between the two monomers.

In classical emulsion polymerization of styrene with a surfactant concentration above the critical micelle concentration, the relationship between the particle number N_p and the initiator $[I]$ and surfactant $[M]$ concentrations²⁰ is given by the following equation:

$$N_p = k \cdot [I]^{2/5} \cdot [S]^{4/5} \quad (13)$$

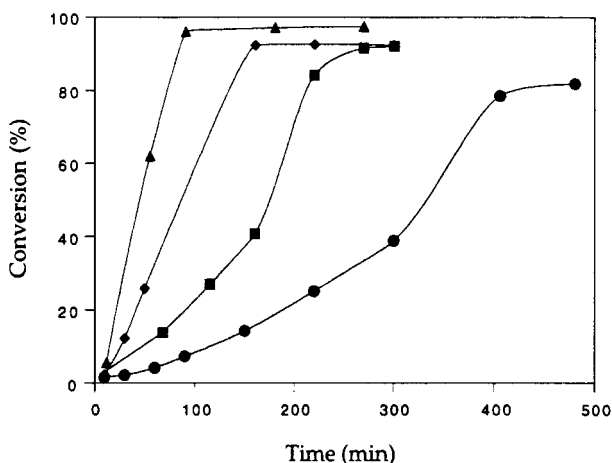


Figure 4 Conversion versus time curves for different emulsion polymerization runs in the presence of VBAH; [VBAH] 10^3 mol L^{-1} : (O, ■) 1.22; (◆) 2.94; (▲) 5.88.

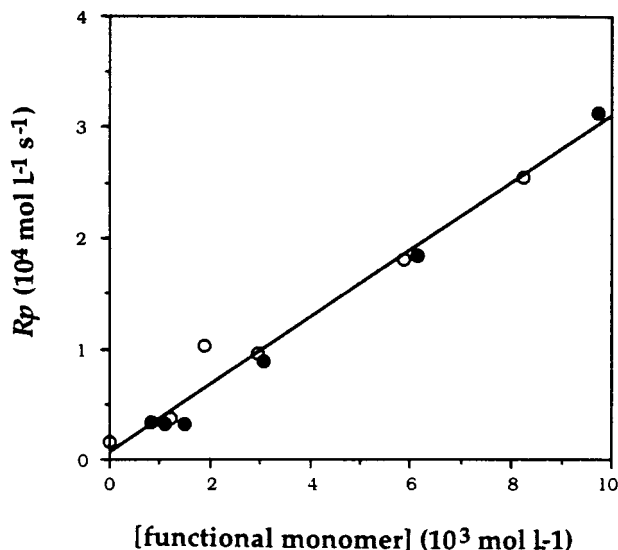


Figure 5 Polymerization rate (R_p) versus the functional monomer concentration; (●) AEMH and (○) VBAH.

In soap-free emulsion copolymerization of styrene in the presence of a functional monomer, the particle stabilization can be ensured by ionic species coming from either the initiator or the ionic monomer. Then, in this case, a relationship can be established taking into account the initiator and functional monomer concentration.

$$N_p = k' \cdot [I]^\alpha \cdot [M]^\beta \quad (14)$$

As explained in the Experimental section, the initiator concentration is high compared to the functional monomer one; therefore, the ionic strength can be considered roughly constant (between 1.9 and $2.8 \times 10^{-2} \text{ mol L}^{-1}$, depending upon the ionic monomer concentration), and its influence is not discussed in this work. The slope of $\ln N_p$ versus the $\ln[M]$ plot (Fig. 6) provides a β coefficient of 1.45. (The determination of α was not investigated, but it is thought that it has a lower influence on the particle number in this case, 0.2 from the literature²⁷.) Similar high values of β were already reported in the case of other ionic comonomers, as shown in Table V. Such a large value indeed confirmed the strong influence of the ionic monomer concentration on the nucleation step: at first, (co)polymerization with the solubilized styrene molecules in the aqueous phase was drastically increased, providing a large number of charged oligomers that precipitated after reaching a critical size and forming precur-

Table IV Influence of Functional Monomer Concentrations on Final Particle Size of Latexes and Conversion

Entry		[Monomer] (10 ³ mol L ⁻¹)	\overline{D}_n (nm)	\overline{D}_w (nm)	\overline{U}	Conv. (%)
VBAH	0	0.00	473	473	1.001	82.5
	1	1.22	272	273	1.004	88.0
	2	1.90	190	192	1.010	90.0
	3	2.94	190	192	1.010	90.0
	4	4.12	152	157	1.030	92.4
	5	5.88	118	119	1.004	96.1
AEMH	6	8.24	115	117	1.020	95.6
	11	0.81	468	469	1.002	90.0
	12	1.51	320	320	1.007	91.8
	13	3.06	186	189	1.016	96.3
	14	6.15	144	145	1.014	97.1
	15	7.47	103	107	1.040	99.5
	16	9.72	85	93	1.090	99.0

sors; the presence of ionic charges resulted in enhanced electrostatic stabilization that then led to more mature particles. It is worth mentioning that ionic monomers with either a styrene or methacrylate polymerizable group similarly affected the kinetics of emulsifier-free copolymerization of styrene, whatever the nature of the ionic charge (sulfate, sulfonate, quaternary ammonium, or amine, as given in Table V). The formation of more mature particles strongly accelerated the polymerization rate because styrene mostly polymerized in the monomer-swollen polymer loci during the growth step.

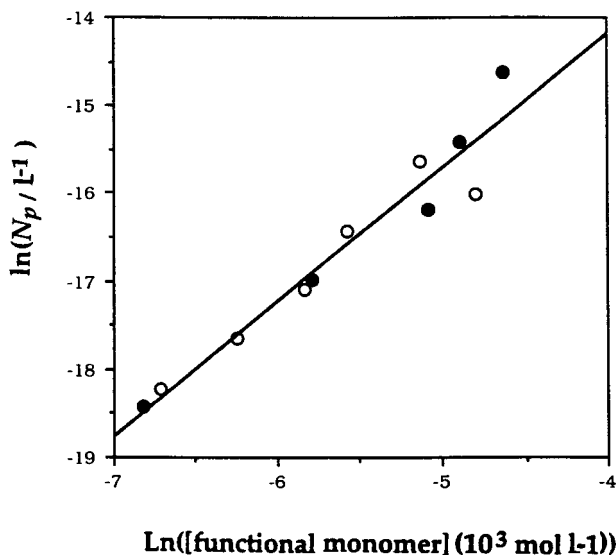


Figure 6 Influence of (○) VBAH and (●) AEMH amount on the number of particles (N_p) created during the nucleation period.

Average Molecular Weight and Weight Distribution

Kinetic Study

Average molecular weights were measured from samples withdrawn during one of the polymerization experiments (run 14, Table VI) at different conversions to examine the influence of the ionic comonomer upon the molecular weight data (Fig. 7). As clearly shown over this conversion range, \overline{M}_n and \overline{M}_w values gave further information: mainly short chains, which might be obtained during the nucleation period, remained constant through the process (\overline{M}_n constant); on the contrary, most long chains were created during this step, which explains the \overline{M}_w increase; and the polydispersity index was much greater than 2, which seemed to indicate that transfer reactions would play a significant role during the reaction. Anyway, it was not possible to glean information on the short or long chains from \overline{M}_n and \overline{M}_w values.

To take advantage of the MWD, Clay and Gilbert²⁹ defined a new function, the cumulative number MWD $\overline{P}(M)$, that was obtained from the GPC trace $G(V_{el})$ and given as

$$\overline{P}(M) = \frac{\overline{W}(M)}{M} = \frac{G(V_{el})}{M \frac{dM}{dV}} \quad (15)$$

where $\overline{W}(M)$ is the weight MWD, V_{el} is the elution volume, and $M(V)$ is the GPC calibration curve. When the calibration curve was linear [i.e., dM/dV

Table V Influence of Type of Ionic Monomer on β Coefficient

Ionic Monomer	β	Reference
Sodium styrene sulfonate	1.41	Kim et al. ²⁸
Sulfoethyl methacrylate	1.9	Shi-Der Juang and Krieger ²⁷
3-(Methacrylamidinopropyl) trimethyl ammonium hydrochloride	1.31	Van Streun et al. ⁵
Vinyl benzyl amine hydrochloride		
Aminoethyl methacrylate hydrochloride	1.45	This work

$dV = aM(V) + b]$ and for high molecular weight values, then

$$\bar{P}(M) = k \times \frac{G(V_{el})}{M^2} \quad (16)$$

where k is an arbitrary constant. This function represents the number MWD and is more suitable than the weight average one, because it permits the exploitation of the weight *distribution*, which is allowed to provide much information on the type of mechanism.

Then, plots of $\ln P(M)$ versus M for different reaction times are reported in Figure 8. It appears that at given times small chains do not seem to vary during the reaction course, but the contribution of long chains gradually increases (in term of chain length). This is in agreement with results plotted in Figure 7, because \bar{M}_n and \bar{M}_w are much more sensitive to short and long polymer chains, respectively.

From this treatment it is possible to deduce transfer rate constants to styrene and to both functional monomers as discussed later.

DISCUSSION

The mechanism of soap-free emulsion polymerization of styrene in the presence of a functional comonomer is quite complex. The incorporation of a

part of the functional monomer in the particles by copolymerization can occur during the nucleation step, where copolymerization of styrene with the comonomer takes place in the water phase. As previously stated by Fitch and Tsai³⁰ and Litchi et al.,³¹ precursors are formed as soon as (co)oligomers reach a critical chain length (usually noticed as a critical degree z_{crit}) and then precipitate; these precursors coagulate with each other until mature particles reach efficient stabilization through the ionic surface charges provided by both the initiator and the functional monomer. Then, in the growth step particles grow until monomer droplets disappear. During the last step (termination period) the main monomer polymerizes within the monomer swollen polymer particles while the remaining functional monomer mostly homopolymerizes in the aqueous phase, then producing polyelectrolytes. More insight concerning the first and second steps can be obtained by studying some pertinent parameters during the polymerization process.

Dealing with the use of functional monomers in soap-free emulsion copolymerization, two main criteria should be fulfilled for producing functional latexes.

1. The functional group must be ionic to efficiently stabilize the particles, as already mentioned according to literature studies.^{5,9}

Table VI Average Molecular Weights as Function of AEMH Concentration Introduced in Recipe

Entry	[Monomer] (mol L ⁻¹)	\bar{M}_n (10 ⁴ g mol ⁻¹)	\bar{M}_w (10 ⁵ g mol ⁻¹)	I_p	
	0	0	5.87	5.65	9.6
AEMH	11	0.81	4.08	2.00	4.9
	13	3.06	3.28	4.11	10.7
	14	6.15	1.91	2.04	10.7
	16	9.72	1.58	1.81	11.5

2. These functional monomers should be able to fairly copolymerize with styrene.⁹

Such criteria are antagonistic because ionic monomers are generally highly water soluble, which makes their incorporation onto the polystyrene particle surface tricky. Consequently, the structure and physicochemical properties of the functional monomer are of paramount importance in emulsion polymerization.

Monomer Reactivity in Water-Phase Polymerization

As illustrated in Figure 2, partitioning between water and styrene reflects the affinity of VBAH (or AEMH) for the water phase. Partition coefficients, derived from eq. (6), were determined such as $K_s = 0.07$ and 0.28 at 25°C for VBAH and AEMH, respectively; this indicated that AEMH was more easily partitioned in the water phase than VBAH, which in turn exhibited a higher affinity for the organic phase. This was consistent with the structure of both monomers. (Styrene derivatives are more hydrophobic than methacrylate ones, as long as the functional group is the same.) However, in the range of the studied concentrations (from 0.02 to 0.4 mol L^{-1}), most of the functional monomer was localized in the aqueous phase. In addition, AEMH was more polymerizable than VBAH, as evidenced by the $k_p/k_t^{1/2}$ ratios reported in Table II. These results were of significant importance, because they suggested that VBAH could be better incorporated into polystyrene chains than AEMH during emulsion polymerization.

Kinetics Mechanism

From eq. (7), giving the polymerization rate (during step II of the Smith–Ewart theory²⁰) as a function of the particle number created during the nucleation period, it was possible to calculate the average number of free radicals per particle (\bar{n}). In one experiment it was checked whether the particle number remained as constant throughout the polymerization as the polymerization rate and \bar{n} during the second step [as illustrated Fig. 9(a–c)]. Furthermore, Figure 10 shows the average number of radicals per particle (\bar{n}) versus the final size of the particles and it clearly appears that \bar{n} increased upon increasing the particle size. However, except for low particle size (100 nm), that is, when high concentrations of functional

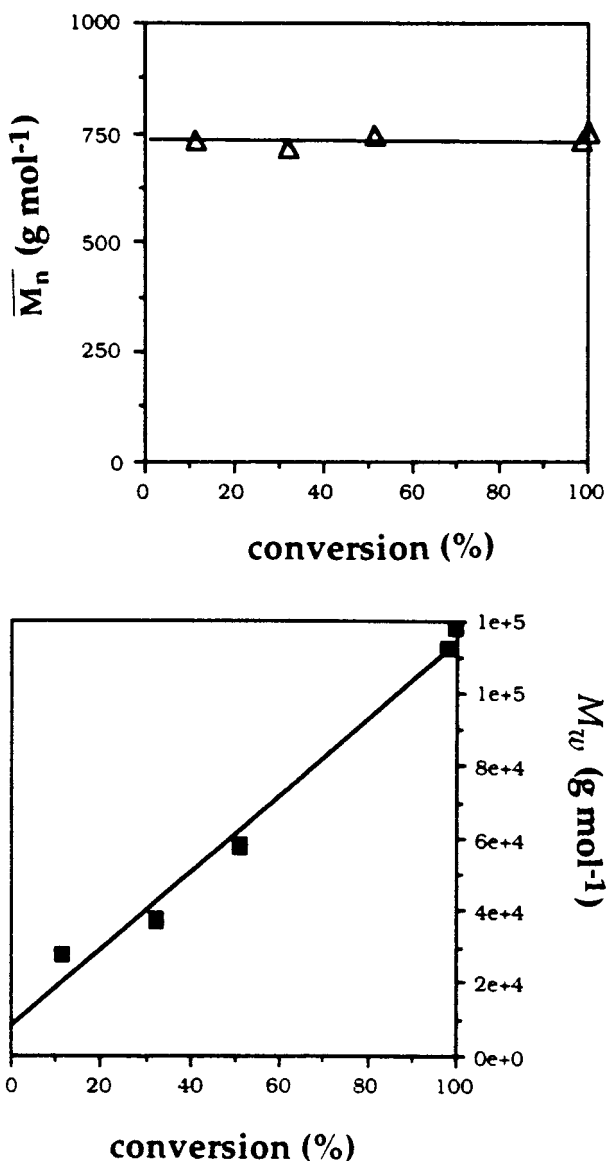


Figure 7 (Δ) Molar (\overline{M}_n) and (\blacksquare) weight (\overline{M}_w) average weight versus conversion. AEMH polymerization, run 14. For details, see text.

monomer were used, the obtained curve suggested that \bar{n} was more likely to depend upon the particle volume. This behavior was consistent with the occurrence of two types of mechanisms during the particle growth: pseudobulk kinetics would prevail for low VBAH (or AEMH) concentrations (providing \bar{n} values ≥ 1) whereas zero-one kinetics (Smith–Ewart case 2²⁰) would only take place for higher monomer concentrations (giving $\bar{n} = 0.5$).

Moreover, it might be assumed that the initiator efficiency becomes 100% with such systems involving a water soluble monomer (VBAH or AEMH), contrary to what was observed in sty-

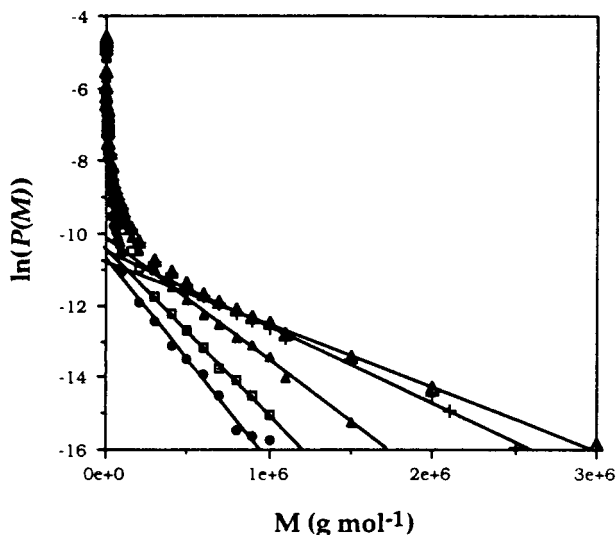


Figure 8 Molar weight distribution [$\ln P(M)$] versus M curves for given conversion; run 14, see Table IV. (●) 11.4%; (□) 32.0%; (▲) 51.3%; (+) 98.6%; (△) 100.0%.

rene emulsion polymerization.³² Such behavior means that capture would be the predominant event during the particle growth compared to aqueous phase termination (because the critical degree of polymerization would be attained rapidly). This could be partially supported by considering that secondary nucleation did not occur during the polymerization of these systems, except for large AEMH or VBAH amounts. The high initiator efficiency could also explain that the overall polymerization rate is independent of the type of ionic monomer.

The MWD study gave further information on the polymerization kinetics, especially on the nucleation period. The very short chains, as expressed by \bar{M}_n (Fig. 7), remained constant over time. These short copolymer chains probably corresponded to oligomers containing styrene and functional monomer created in the aqueous phase during the nucleation period, until they precipitated when they reached a critical size degree (z_{crit}).

In addition, Figure 8 shows the evolution of the longer chains versus conversion after treatment using the Clay and Gilbert method.²⁹ The curves were linear in the high molecular weight domain that is typical of systems in which the termination mechanism is dominated either by combination or transfer (or both).³² However, interestingly, the cumulative MWD changed strongly upon conversion until it reached a limit (the slope of the curve tends to constant value). This large evolution of the MWD means that transfer to functional mono-

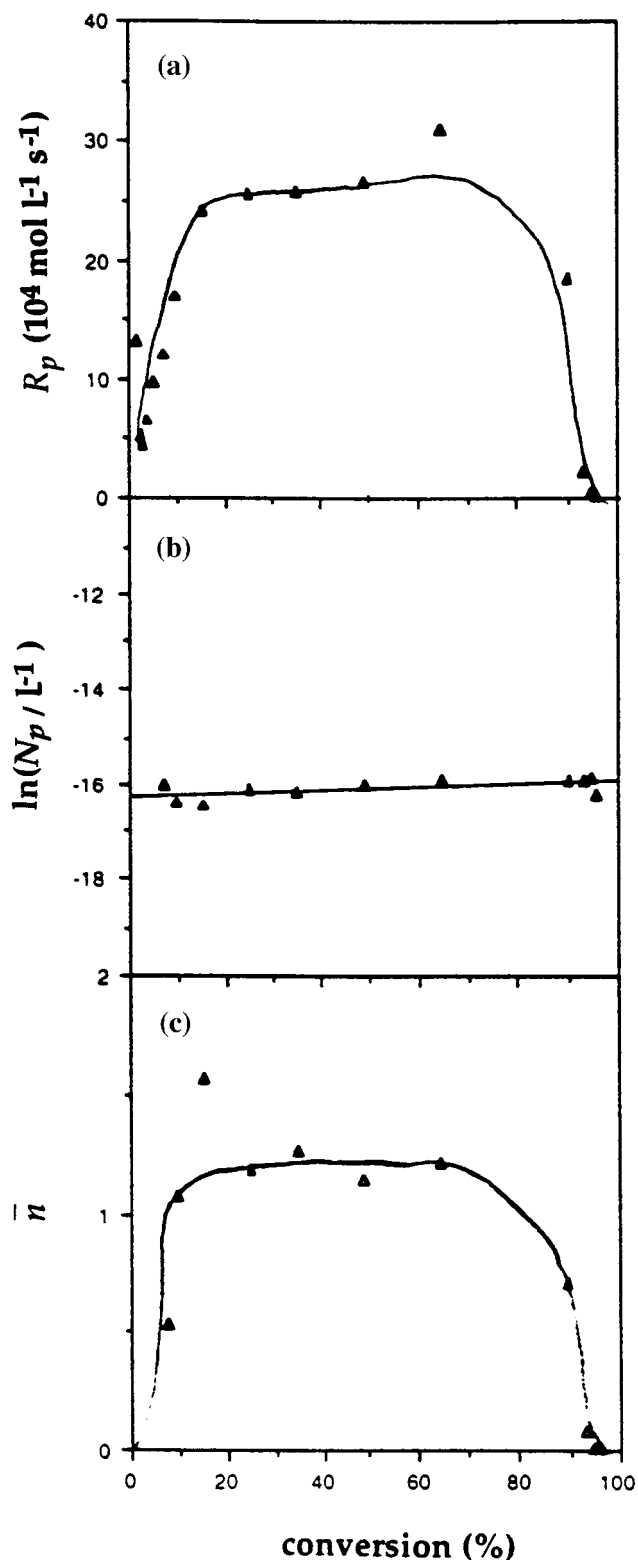


Figure 9 (a) Polymerization rate (R_p) versus conversion for one experiment; VBAH polymerization, run 6; see Tables III and IV for the recipe. (b) Particle number (N_p) versus conversion for the same run. (c) Average radical number (\bar{n}) versus conversion (same run).

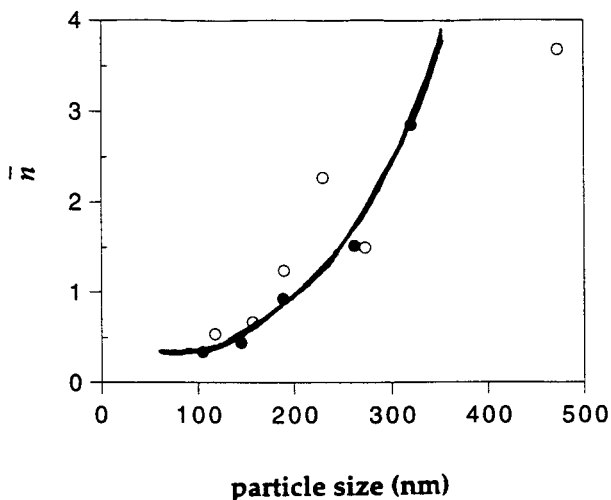


Figure 10 Plot of the average radical number (\bar{n}) versus particle size; (●) AEMH and (○) VBAH.

mers (VBAH or AEMH) is the predominant chain-stopping event. The chain length at high conversion, which should only correspond to styrene emulsion polymerization, exhibited values not far from those usually reported in soap-free systems of this monomer (around a 10^5 order of magnitude).³³

From this preliminary treatment, it seems possible to more accurately describe the transfer mechanism of the functional monomers.

Transfer Mechanism

Chain transfer reaction to the functional monomer or to the polymerized one can occur in three different loci: in the aqueous phase, at the interface, or in the particles.

As already mentioned, the present functional monomers were predominantly water soluble, as pointed out with the partition coefficients reported in Figure 2, at very low comonomer amounts. Hence, transfer to the monomer should occur in the aqueous phase but not in the particles. Furthermore, the incorporation of the functional monomer should not occur after the nucleation period. This will be described in a second article.³⁴ Then, the thought is that the functional monomer is not the chain transfer agent for the polymerization in the particles.

Vidal et al.³⁵ demonstrated that a bimodal MWD was found when the transfer agent was *in* the particles. Indeed, very low molecular weights were formed because the transfer agent acted in the particles. When it was totally consumed, high

molecular weights were then formed. On the contrary, with a more hydrophilic transfer agent, such as thioglycolic acid, this molecule was located at the interface of the particle and was then consumed more slowly throughout all the polymerization. Chain transfer occurred continuously, then forming a unimodal distribution. In our case, as indicated with the evolution of molecular weight vs. conversion, the transfer seemed to take place during a large part of the polymerization time.

It can be postulated that oligomers located at the interface could play a major role in the chain transfer process with the growing chains diffusing in the particles. Such a hypothesis seems relevant as long as the following holds true.

The transfer effect depends on the amount of monomer incorporated at the latex surface. The molecular weights of polymer latexes produced with various AEMH concentrations are shown in Table VI: the higher the AEMH incorporation yield, the lower the observed molecular weight. In that case, because more and small particles were formed, the growing chains during their diffusion in the particle were able to reach the particle shell more easily; thus chain transfer to the ionic oligomers would be favored.

The transfer effect also depends on the conversion, because when the particles become more and more viscous as they are growing, the macromolecule chains propagating in the particle are less likely to reach the surface and terminate by transfer.

A scheme of the chain transfer process is depicted in Figure 11. Radicals created by the initiator begin the aqueous phase polymerization. The copolymer chain, propagating in the aqueous phase, can either terminate by transfer to the monomer and stay in water or enter a particle when reaching the critical chain length z_{crit} . The growing chains in the particle are more likely to terminate by transfer to the oligomers containing functional monomers at the interface. Finally, the new radical, anchored at the particle interface, cannot exit but is able to reinitiate a chain growing in the particle.

Transfer Rate Constant for Functional Monomers

Transfer rate constants for the two functional monomers can be determined, if considering that they only act as a transfer agent (which should be the case, considering that it is the oligomers at the interface that transfer). Gilbert³³ derived

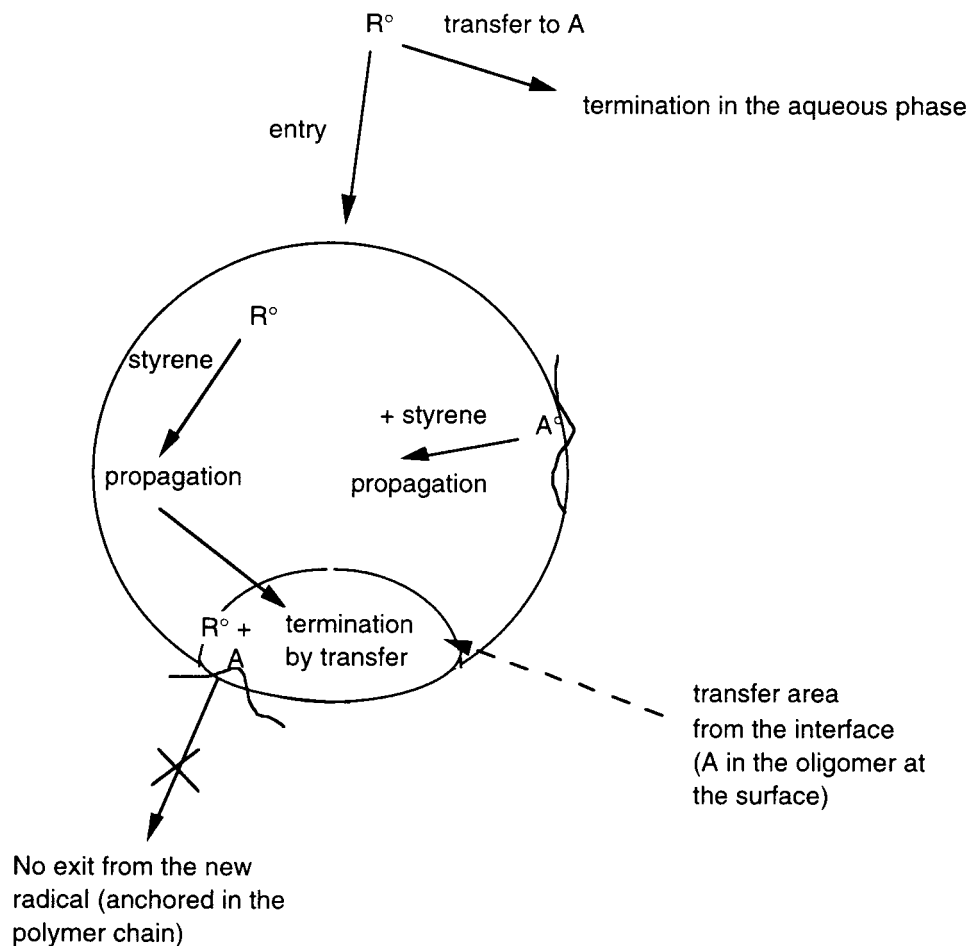


Figure 11 Mechanism of transfer to the functional monomer incorporated in the oligomer at the surface of the particle.

an expression to estimate the transfer constant for the functional monomer $k_{tr,A}$ (considered as a transfer agent) as a function of the MWD, such as,

$$\lim_{M \rightarrow \infty, [I] \rightarrow 0} P(M) = B \exp \left\{ - \frac{k_{tr,S}[S] + k_{tr,A}[A]}{k_p[S]} \frac{M}{M_0} \right\} \quad (17)$$

where M_0 is the molecular weight of the monomer, $[S]$ is the concentration of styrene in the particle, $[A]$ is the concentration of functional monomer, and B is a proportionality constant. As expressed by this equation, such an estimation is only possible for high molecular weights and low initiator concentration compared to the main monomer content, which is the case in our conditions (recipe Table III), to make sure that the only termination by transfer occurs.

Although instantaneous MWDs should be used for determining the transfer constant, this calculation was performed with the final ones for VBAH and AEMH; indeed, as shown in Figure 12, when the functional monomer was not transfer active anymore, the slope of the straight line corresponding to the higher MWD (plotted in Fig. 8) was constant until the end of the polymerization. A plot of $-(k_{tr,S}[S] + k_{tr,A}[A])/k_p[S]$ versus the monomer ratio $[A]/[S]$ was obtained as illustrated in Figure 13. It was considered that the apparent propagation rate constant k_p , during the growth step (polymerization in the particles), was equal to that of styrene ($k_p = 4.8 \times 10^2 \text{ L mol}^{-1} \text{ s}^{-1}$ at 70°C),²¹ because a major part of the functional monomer was in the aqueous phase. From the curves plotted in Figure 13, transfer rate constants $k_{tr,S}$ and $k_{tr,A}$ for the main monomer (i.e., styrene) and the two functional monomers, respectively, can be deduced as reported in Table

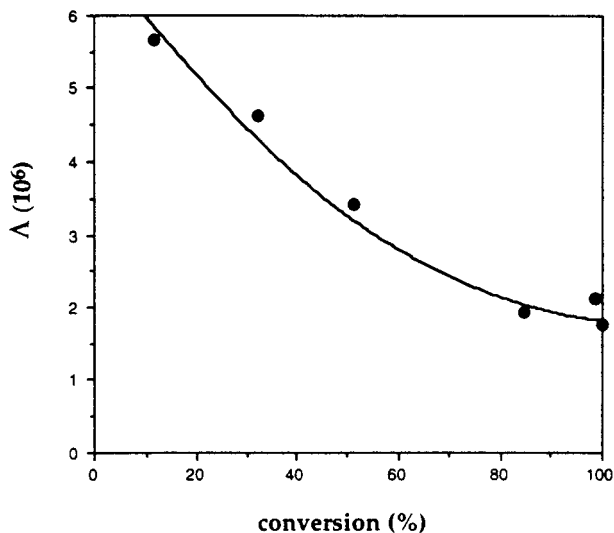


Figure 12 $\ln P(M)$ versus $(\Lambda)M$ curve slopes for high molecular weight values (run 14).

VII. From these values, the following comments may be emphasized.

The transfer rate constant $k_{tr,S}$ for styrene was quite reliable from one to the other copolymerizing system. Further, the obtained value is in good agreement with the one reported by Tobolsky and Offenbach,³⁶ $2.9 \times 10^{-2} \text{ L mol}^{-1} \text{ s}^{-1}$ at 70°C .

Transfer rate constants $k_{tr,A}$ were set very high, and there was no significant difference according to the nature of the functional monomer. These values were about 1000 times higher than for sty-

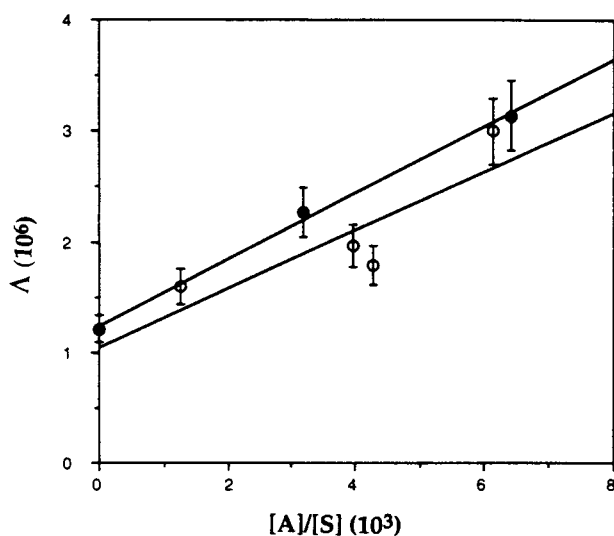


Figure 13 $(\Lambda) - (k_{tr,S}[S] + k_{tr,A}[A])/k_p[S]$ versus the monomer ratio $[A]/[S]$ for the two monomers; (●) AEMH and (○) VBAH.

Table VII Transfer Rate Constant for Main Monomer, Styrene, and Functional Ones, VBAH and AEMH

Monomer	$K_{tr,S}$ ($\text{L mol}^{-1} \text{ s}^{-1}$)	$k_{tr,A}$ ($\text{L mol}^{-1} \text{ s}^{-1}$)
AEMH	4.6×10^{-2}	11.1
VBAH	3.9×10^{-2}	9.9

Determined by the Clay and Gilbert method.²⁹

rene, that is to say, similar to the transfer rate constant for a conventional active transfer agent such as quaternary amine or mercaptan.³⁷ This could suggest that the transfer reaction would involve a labile proton such as in the amino function, which is in equilibrium between the protected form (hydrochloride) and the nonprotected one (amino). This would assume the strong chain transferring activity of the nonprotected form, although in our case at the pH of the polymerization medium (around pH 4), the amount of unprotected amine is less than 0.5%. It was indeed reported that vinyl benzyl amine exhibited a high chain transfer activity in both solution and emulsion polymerization.²⁶ Furthermore, in the same work,²⁶ the monomer protected with a trifluoroacetamide in homopolymerization provided a molecular weight similar to the one with styrene, which again suggests that the only labile amino function is responsible for the transfer.

In conclusion, this method should provide reliable results concerning the chain transfer reaction originated from functional monomers when used in an emulsion process.

CONCLUSION

The aim of this work was to synthesize latexes bearing amino surface charges using soap-free batch emulsion polymerization of styrene as the main monomer, V50 as an initiator, and two cationic monomers, AEMH and VBAH.

The influences of several parameters were studied, and the main results may be emphasized.

1. Comparison of the partition coefficient of both monomers showed a higher hydrophilicity for AEMH than for VBAH, which was explained by their structure. Furthermore, solution polymerization in water provided $k_p/k_i^{1/2}$ values of 4.0 and 1.75 (L mol^{-1}

- $s^{-1})^{1/2}$ for AEMH and VBAH, respectively; indeed, AEMH was expected to exhibit a higher homopolymerizability than VBAH due to the greater reactivity of methacrylate compared to that of vinylic functions.
- The influence of the functional monomer concentration on the emulsion copolymerization rate and particle number was found to be quite similar for both monomers. It was also evidenced that the presence of very small amounts of functional monomer strongly affected the particle size because of the electrostatic stabilization conferred by the cationic groups to the growing particles. This caused a decrease of the final particle size upon increasing the monomer concentration. In addition, the average radical number \bar{n} value was also found to be drastically affected by the functional monomer concentration in relation to the volume of the particle; indeed, it reached 0.5, a value corresponding to the so-called zero-one conditions for a particle size smaller than 100 nm.
 - Transfer rate constants to styrene and functional monomers at 70°C were determined with the knowledge of the MWD. The transfer rate constant for styrene at 70°C was close to recent literature values and those for the two functional monomers were found to be very large, which suggests that chain transfer reactions occur from the labile hydrogen coming from the partially unprotected amino function.

Finally, it is interesting to note that the synthesis of cationic hydrophobic latexes (polystyrene), upon using a ionic monomer in the polymerization, led to the formation of a population of small polymer chains that remain mainly located at the outer shell of the particle during and after particle growth.⁹ This was confirmed through the surface characterization of VBAH containing batch latexes that showed that a large proportion of cationic charges was indeed available at the surface.¹⁵

Based on this kinetic study, further work was devoted to the colloidal and surface properties of these cationic latexes according to the type of functional monomer. The results are described in the second part of this series.

The authors would like to thank Flavien Melis

(LMOPS-CNRS-Solaize) for his contribution to the measurements of molecular weights.

REFERENCES

- P. Cousin and P. Smith, *J. Appl. Polym. Sci.*, **54**, 1631 (1994).
- J. W. Goodwin, R. H. Ottewill, R. Pelton, G. Vianello, and D. E. Yates, *Brit. Polym. J.*, **10**, 173 (1978).
- J. W. Goodwin, R. H. Ottewill, and R. Pelton, *Colloid Polym. Sci.*, **257**, 61 (1979).
- J. W. Goodwin, J. Hearn, C. C. Ho, and R. H. Ottewill, *Brit. Polym. J.*, **5**, 347 (1973).
- K. H. Van Streun, W. J. Belt, P. Piet, and A. L. German, *Eur. Polym. J.*, **27**, 931 (1991).
- W. T. Ford, H. Yu, J. J. Lee, and H. El-Hamshary, *Langmuir*, **9**, 1698 (1993).
- Y. Ionmata, T. Wada, H. Handa, K. Fujimoto, and H. Kawaguchi, *J. Biomater. Sci. Polym. Ed.*, **5**, 293 (1994).
- Th. Delair, C. Pichot, and B. Mandrand, *Colloid Polym. Sci.*, **272**, 72 (1994).
- R. Arshady, *Biomaterials*, **14**, 5 (1993).
- C. Pichot, B. Charleux, M.-T. Charreyre, and J. Revilla, *Macromol. Symp.*, **88**, 71 (1994).
- A. Guyot and K. Tauer, *Adv. Polym. Sci.*, **111**, 45 (1994).
- W. T. Carvill and R. M. Fitch, *J. Colloid Interface Sci.*, **67**, 204 (1978).
- R. A. Wessling, in *Science and Technology of Colloids*, G. W. Poehlein, R. H. Ottewill, and G. W. Goodwin, Eds., Martinus Nijhoff Publishers, The Hague, 1993, p. 393.
- H. Kawaguchi, H. Hoshino, and Y. Ohtsuka, *J. Appl. Polym. Sci.*, **26**, 2015 (1981).
- Th. Delair, V. Marguet, C. Pichot, and B. Mandrand, *Colloid Polym. Sci.*, **272**, 962 (1994).
- M. C. L. Maste, A. P. C. Van Velthoven, W. Norde, and J. Lyklema, *Colloids Surfaces Part A*, **83**, 255 (1994).
- J. Lokaj, D. Doscocilova, and F. Hrabak, *Macromol. Chem.*, **185**, 1177 (1984).
- R. Arshady, *J. Macromol. Sci. Rev. Macromol. Chem. Phys.*, **32**, 101 (1992).
- L. Veron, M.-C. de Bignicourt, Th. Delair, C. Pichot, and B. Mandrand, *J. Appl. Polym. Sci.*, **60**, 235 (1996).
- W. V. Smith and R. H. Ewart, *J. Chem. Phys.*, **16**, 592 (1948).
- M. Buback, R. G. Gilbert, R. A. Hutchinson, B. Klumperman, F.-D. Kuchta, B. G. Manders, K. F. O'Driscoll, G. T. Russell, and J. Schweer, *Macromol. Chem. Phys.*, **196**, 3267 (1995).
- P. Maruthamuthu, *Makromol. Chem., Rapid Commun.*, **1**, 23 (1980).

23. H. A. S. Schoonbrood, Ph.D. dissertation, Technical University, Eindhoven, 1994.
24. Anon., *Product Bulletin V-50*, Wako Chemicals, USA, 1985.
25. B. M. Soghomonyan and N. M. Beilerian, *Armen. Chim. Zh.*, **31**, 567 (1978).
26. M. T. Charreyre, V. Razafindrakoto, L. Veron, Th. Delair, and C. Pichot, *Macromol. Chem. Phys.*, **195**, 2141 (1994).
27. M. Shi-Der Juang and I. M. Krieger, *J. Polym. Sci.: Polym. Chem. Ed.*, **14**, 2089 (1976).
28. J. H. Kim, M. Chainey, M. S. El-Aasser, and J. W. Vanderhoff, *J. Polym. Sci., Part A: Polym. Chem.*, **27**, 3187 (1989).
29. P. A. Clay and R. G. Gilbert, *Macromolecules*, **28**, 552 (1995).
30. R. M. Fitch and C. H. Tsai, in *Polymer Colloids*, Fitch, Ed., Plenum Press, New York, 1971.
31. G. Lichti, R. G. Gilbert, and D. H. Napper, *J. Polym. Sci.: Polym. Chem. Ed.*, **21**, 20 (1983).
32. D. I. Christie and R. G. Gilbert, *Macromol. Chem. Phys.*, **197**, 403 (1996).
33. R. G. Gilbert, *Emulsion Polymerization: A Mechanistic Approach*, Academic Press, London, 1995.
34. F. Cornier, F. Ganachaud, A. Elaissari, and C. Pichot, *J. Appl. Polym. Sci.*, to appear.
35. F. Vidal, A. Guyot, and R. G. Gilbert, *Macromol. Chem. Phys.*, to appear.
36. A. V. Tobolsky and J. Offenbach, *J. Polym. Sci.*, **16**, 311 (1955).
37. C. H. Bamford and E. F. T. White, *Trans. Faraday Soc.*, **34**, 268 (1958).